ELSEVIER

Coordination Chemistry Reviews
216–217 (2001) 363–382

COORDINATION CHEMISTRY REVIEWS

www.elsevier.com/locate/ccr

Similarities and differences between the isoelectronic Gd^{III} and Eu^{II} complexes with regard to MRI contrast agent applications

Éva Tóth, László Burai, André E. Merbach *

Institut de Chimie Minérale et Analytique, Université de Lausanne, BCH, CH-1015 Lausanne, Switzerland

Received 8 August 2000; received in revised form 27 November 2000; accepted 19 December 2000

Contents

Abstract

In solution, the $[Eu^{II}(DTPA)(H_2O)]^{3-}$, $[Eu^{II}(DOTA)(H_2O)]^{2-}$, $[Eu^{II}(ODDM)]^{2-}$ and $[Eu^{II}(ODDA)(H_2O)]$ complexes are less stable towards oxidation than $[Eu(H_2O)_8]^{2+}$, as shown by their redox potentials ($E_{1/2} = -1.35$, -1.18, -0.92, -0.82 and -0.63 V versus Ag | AgCl electrode, respectively) ($DTPA^{5-}$ = diethylenetriamine-*N*,*N*,*N*′,*N*″,*N*″-pentaacetate, $DOTA^{4-}$ = 1,4,7,10-tetraazacyclododecane-1,4,7,10-tertraacetate, $ODDM^{4-}$ = 1,4,10,13-tetraoxa-7,16-diazacyclooctadecane-7,16-dimalonate and $ODDA^{2-}$ = 1,4,10,13-tetraoxa-7,16-diazacyclooctadecane-7,16-diacetate).

* Corresponding author. Tel.: +41-21-6923871; fax: +41-21-6923875.
E-mail address: andre.merbach@icma.unil.ch (A.E. Merbach).

PII: S0010-8545(01)00312-5

In the solid state, the $[Eu^{II}(DTPA)(H_2O)]^{3-}$ complex is nine-coordinate with one inner-sphere water molecule. Its structure is practically identical with that obtained for the Sr^{II} analogue, and very similar to that of $[Gd(DTPA)(H_2O)]^{2-}$ (the bond angles are equal, but the metal–nitrogen and metal–oxygen bond distances are longer for the Eu^{II} than for the Gd^{III} complex).

In contrast to similar Gd^{III} poly(amino carboxylate) complexes in general, the rate of water exchange for $[Eu^{II}(DTPA)(H_2O)]^{3-}$ and $[Eu^{II}(ODDA)(H_2O)]$ is only slightly diminished as compared to the aqua ion ($k_{ex}^{298} = 1.3 \times 10^9$, 0.43×10^9 and 4.4×10^9 s^{-1} for $[Eu^{II}(DTPA)(H_2O)]^{3-}$, $[Eu^{II}(ODDA)(H_2O)]$ and $[Eu(H_2O)_8]^{2+}$, respectively). The mechanism of the water exchange, as evidenced by the activation volumes, is limiting associative (**A**) for $[Eu(H_2O)_8]^{2+}$ ($\Delta V^{\#} = -11.3$ $cm^3\,mol^{-1}$), dissociative interchange ($\mathbf{I_d}$) for $[Eu^{II}(DTPA)(H_2O)]^{3-}$ ($\Delta V^{\#} = +4.5$ $cm^3\,mol^{-1}$) and associative interchange ($\mathbf{I_a}$) for $[Eu^{II}(ODDA)(H_2O)]$ ($\Delta V^{\#} = -3.9$ $cm^3\,mol^{-1}$).

Electron spin relaxation is faster for the Eu^{II} complexes studied than for corresponding Gd^{III} analogues. Proton relaxivities of $[Eu(H_2O)_8]^{2+}$, $[Eu^{II}(DTPA)(H_2O)]^{3-}$ and $[Eu^{II}(ODDA)(H_2O)]$ are lower in the proton Larmor frequency range 0–200 MHz than those of the analogue Gd^{III} chelates. The analysis of the NMRD profiles reveals that, beside fast rotation, for $[Eu(H_2O)_8]^{2+}$ the extremely fast water exchange rate, whereas for $[Eu^{II}(DTPA)(H_2O)]^{3-}$ and $[Eu^{II}(ODDA)(H_2O)]$ fast electron spin relaxation also limits proton relaxivity.

Keywords: Gd^{III}; Eu^{II}; MRI contrast agents; Redox responsive agents; NMR; EPR; X-ray solid state structure

1. Introduction

In the last decade, magnetic resonance imaging (MRI) has evolved into one of the most powerful techniques in clinical medical diagnostics. Its strong expansion has prompted the development of a new class of pharmacological products, called contrast agents, designed for administration to patients in order to enhance the contrast between normal and diseased tissue or to indicate organ function or blood flow. The majority of the approved contrast agents are Gd^{III} chelates, due to their high paramagnetism and relatively slow electron spin relaxation [1].

The efficiency of a contrast agent is given by its proton relaxivity. The proton relaxivity, r_1, is the proton relaxation rate enhancement in the presence of the paramagnetic agent compared to a diamagnetic environment, normalized by the concentration of the paramagnetic agent. For paramagnetic metal complexes, the relaxivity is the sum of outer- and inner-sphere contributions [2]. Outer-sphere relaxivity arises from long-range dipolar interactions between the paramagnetic metal ion and the protons of the bulk water in the vicinity of the complex and is determined by the relative diffusional motions of the unbound water molecules and the paramagnetic ion [3]. The inner-sphere relaxivity contribution, arising from the proton of the exchangeable water molecule(s) bound in the inner coordination sphere of the metal ion, is influenced by correlation times involving rotation, proton exchange, and electronic relaxation, as well as the number of water molecules bound in the inner coordination sphere (Fig. 1).

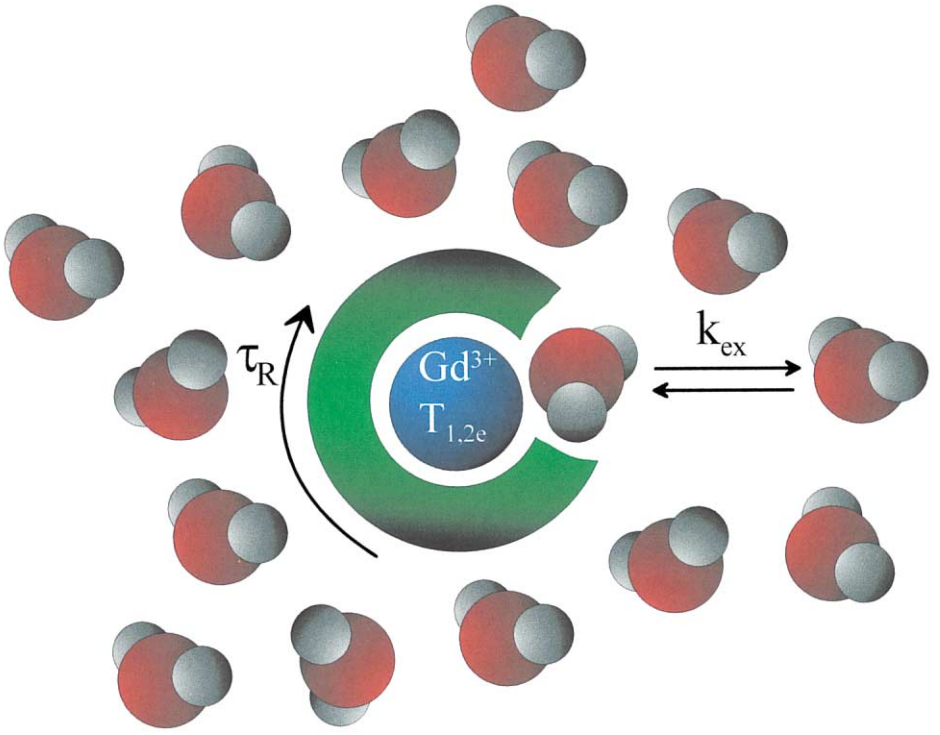

Fig. 1. Schematic representation of a Gd^{III} complex having one water molecule in the inner coordination sphere. The chelate is surrounded by bulk water. The parameters that determine the inner-sphere proton relaxivity are the rotational correlation time, τ_R, the water/proton exchange rate, k_{ex}, and the longitudinal and transverse relaxation rates of the Gd^{III} electron spin, $1/T_{1,2e}$.

Water molecules that are not directly bound in the first coordination sphere may also remain in the proximity of the paramagnetic metal for a relatively long time, mainly due to hydrogen bridges to the ligand (e.g. to its carboxylate or phosphonate groups). The relaxivity contribution originating from these interactions is called second sphere relaxivity. The three different types of water molecules (outer-, inner- and second-sphere water) which lead to the three different relaxation contributions are represented in Fig. 2 by a molecular dynamic simulation picture obtained for $[Gd(DOTA)(H_2O)]^-$ in aqueous solution.

It is mainly the inner-sphere relaxivity term that can be considerably increased by appropriate modification of the influencing parameters. Thus for the new generation agents of higher efficiency (higher relaxivity), the inner-sphere term becomes more important and represents the major contribution to the overall proton relaxation rate. In order to visualize the effect of the different influencing parameters, Fig. 3 shows simulated inner-sphere proton relaxivities as a function of the proton exchange rate and of the rotation at different fields and at different values of the electronic relaxation rate.

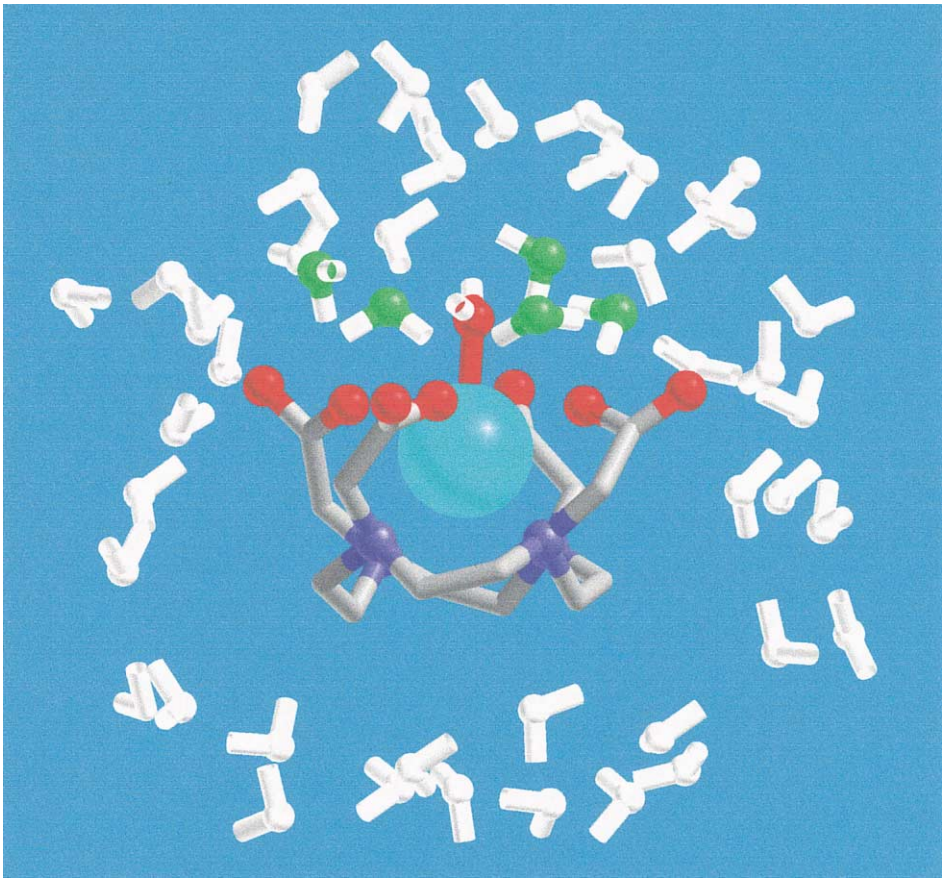

Fig. 2. Different types of water molecules around a Gd^{III} complex, as obtained by molecular dynamics simulation of $[Gd(DOTA)(H_2O)]^-$ in aqueous solution. The inner-sphere water molecule is directly coordinated to the metal (its oxygen is red). Second sphere water molecules are on the hydrophilic side of the complex, hydrogen-bonded to the carboxylate oxygens (their oxygens are green). Outer sphere or bulk water molecules have no preferential orientation (shown in white). Bulk water molecules in front and behind the complex have been removed for clarity [3].

There are three principal techniques generally used to determine the parameters that affect proton relaxivity of MRI contrast agents. Nuclear magnetic resonance dispersion (NMRD) measures proton relaxation rates as a function of magnetic field and, in principle, gives information on all the influencing parameters. This also represents a disadvantage: the separation of the different effects is often problematic which necessitates their independent determination [4]. EPR can be used to access electronic relaxation rates. ^{17}O-NMR is an efficient technique for studying water exchange parameters; the oxygen atom of the coordinated water molecule is directly bound to the paramagnetic ion and is thus a more sensitive antenna than protons. The ideal approach is to use all the three techniques to characterize relaxation parameters of MRI contrast agents [5].

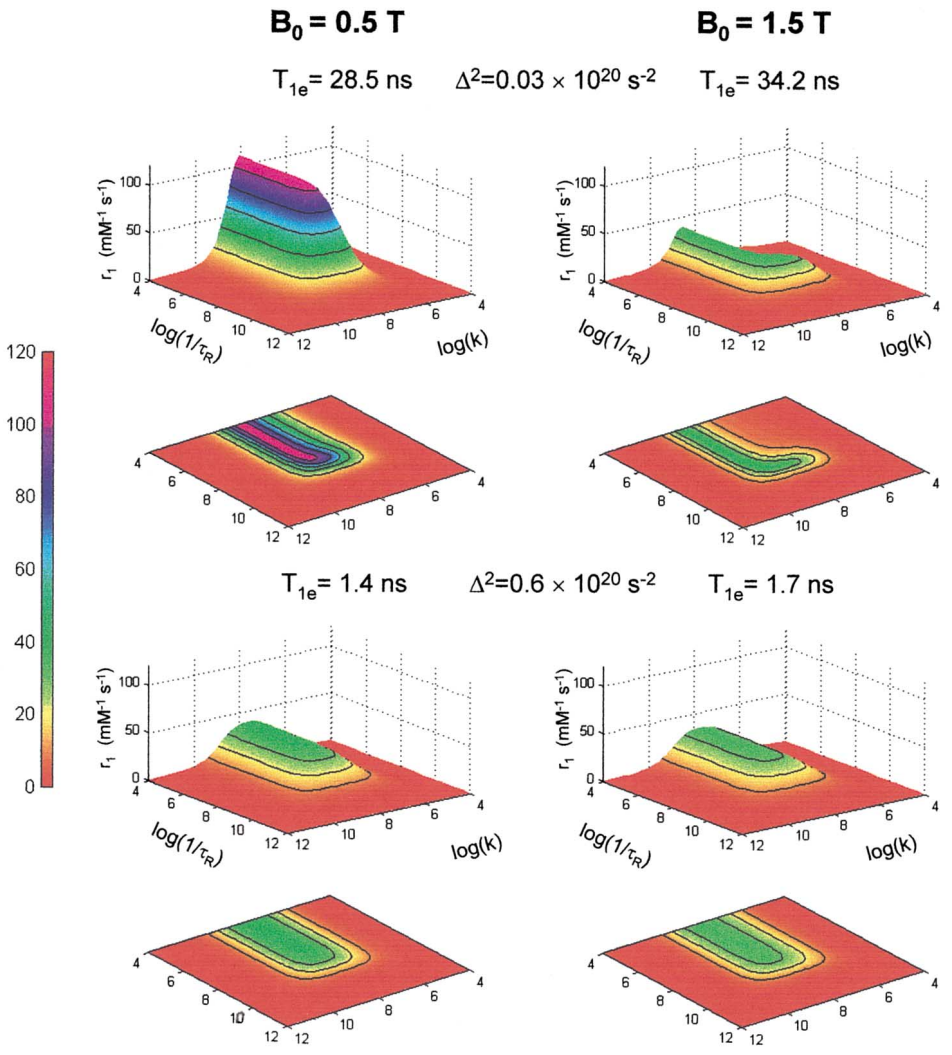

Fig. 3. Inner-sphere ^{1}H relaxivities calculated as a function of $1/\tau_R$ and k_{ex} at B_0 of 0.5 and 1.5 T and plotted as 3D- and contour plots. In all cases the correlation time for the modulation of the ZFS, τ_v, was 1×10^{-12} s^{-1}.

Current contrast agents have much lower relaxivities than the theoretically attainable values (Fig. 3). For monomer Gd^{III} complexes, the relaxivity is mainly limited by fast rotation. It is relatively straightforward to slow down rotation by using high molecular weight compounds. New approaches have involved linking the Gd^{III} chelate either covalently [6] or non-covalently [7] to a macromolecule. However, very often rapid internal motions prevent relaxivities from attaining maximum values [8]. Furthermore, for these slowly rotating high molecular weight

compounds slow proton/water exchange also starts to limit relaxivity [9]. Unfortunately, the optimization of the proton or water exchange rate is not as evident as slowing the rotation. In the last few years, we have accumulated a large body of knowledge by determining the rate and mechanism of water exchange for a high number of Gd^{III} chelates [5,10–12]. All approved and the majority of the potential Gd^{III}-based contrast agents are nine-coordinate complexes with one inner-sphere water molecule. For series of similar nine-coordinate Gd^{III} complexes with dissociatively activated water exchange the exchange rate has been found to be primarily influenced by the steric crowding in the inner coordination sphere and by the overall charge of the complex. It has also been observed that changes outside the inner coordination sphere have negligible effect on the water exchange rate and mechanism. Accordingly, the same Gd^{III} chelate has the same water exchange rate independently if it is a monomer compound or part of a macromolecule [8,9]. Some clues have been proposed to increase the water exchange rate on Gd^{III} chelates, such as using complexes that are present in an equilibrium between different hydration states, or increasing the overall charge of the molecule. Unfortunately, these attempts had only limited success [13].

2. Specific contrast agents — reporters of the biological environment

While MRI has been primarily used to generate anatomical images, current developments go in the direction of visualizing the physical–chemical state of tissues. These applications need specific contrast agents which are capable of producing images that depend on given physico-chemical parameters of the tissue, i.e. which are reporters of the biological environment. Consequently, beside the search for high relaxivity compounds which has been in the front of contrast agent development since their first use, current research is focused on these responsive or ''smart'' contrast agents. The most important physiological parameters to be monitored by MRI involve partial oxygen pressure, pH, temperature, ion distribution in the intra- and extracellular space, metabolite concentration or enzymatic activity. One of the few examples for a ''smart'' contrast agent published so far is the Gd^{III} complex of the galactopyranose derivatized DOTA which can act as a reporter for the β-galactosidase enzyme. This enzyme removes the galactopyranose unit, which blocked the water coordinating site, from the chelate thus produces a higher relaxivity state [14].

The oxygen partial pressure, pO_2, is particularly significant in metabolic processes of cells, and plays an important role in many pathologies (ischemic diseases, strokes, tumors). Accurate and localized measurements of the oxygen concentration are also desirable for differentiation between venous and arterial blood or for cerebral mapping of task activation. So far only invasive methods existed involving oxygen sensitive electrodes which have to be placed directly in the blood or tissue and can only offer pO_2 from few body points.

The simplest design of a pO_2 responsive, MRI contrast agent is based on metal complexes whose metal ion can be reduced or oxidized depending on the biological

environment, and the two oxidation forms have different relaxation properties. Thus the two redox states influence the proton relaxation of the surrounding protons in a different extent, resulting in different image intensities. The adducts formed between Mn^{III}/Mn^{II} tpps complexes and poly-β-cyclodextrine have been recently reported to have considerably different relaxivities depending on the redox state of the metal, itself determined by the partial oxygen pressure of the solution [15] (tpps = 5,10,15,20-tetrakis-(*p*-sulfonatophenyl porphinate).

The Eu^{III}/Eu^{II} system could also be a good candidate, since Eu^{II} has seven unpaired electrons in an ^8S ground state and is isoelectronic with Gd^{III}. Thus the Gd^{III} and Eu^{II} complexes can be expected to have similar proton relaxivities, whereas Eu^{III} is a very poor relaxing agent. A potential application of Eu^{III}/Eu^{II} complexes as redox responsive MRI probes requires the control of both the redox and thermodynamic stability of the complex in the lower oxidation state. In this perspective, we have started to explore the coordination and redox chemistry of Eu^{II} chelates [16–18]. Beside the interest in Eu^{III}/Eu^{II} systems as potential redox responsive agents, Eu^{II} complexes offer a good possibility to investigate the effects of the water exchange rate and electronic relaxation on the proton relaxivity when they are much different from those of the corresponding Gd^{III} analogues. Since it is rather difficult to considerably increase water exchange rate, or even more problematic to influence electron spin relaxation on Gd^{III} poly(amino carboxylates), changing the metal to a fast exchanging one and modify the electronic properties will provide valuable information. In particular, it has been proposed for Gd^{III} compounds with long (nanosecond) rotational correlation times that electronic relaxation may become a limiting factor for proton relaxivity at medium fields (20 MHz). Studying the analogous Eu^{II} complexes can help illuminate this area of research. Therefore, these studies allow us to better understand the different mechanisms governing proton relaxivity of paramagnetic metal complexes in general and then to design more efficient contrast agents for medical MRI. In this paper we review the proton and electronic relaxation properties, the thermodynamic and redox stability, as well as the solid state structure of Eu^{II} complexes in the perspective of their potential use as redox responsive contrast agents in MRI. In such a review, it is inevitable to make comparison to complexes of the isoelectronic Gd^{III}, for which a large body of data is available. The ligands investigated involve DTPA, the chelating agent of the first approved and most widely used MRI contrast agent, $[Gd(DTPA)(H_2O)]^{2-}$, as well as the macrocyclic poly(amino carboxylate) ligands ODDA and ODDM ($ODDA^{2-}$ = 1,4,10,13-tetraoxa-7,16-diazacyclooctadecane-7,16-diacetate; $ODDM^{4-}$ = 1,4,10,13-tetraoxa-7,16-diaza-cyclooctadecane-7,16-dimalonate; see Scheme 1). These latter ligands have been selected on the basis of the high stability of their Sr^{II} complexes [19]. Eu^{II} is intermediate in size between Ca^{II} and Sr^{II} (ionic radii are 125, 112 and 126 pm for Eu^{II}, Ca^{II} and Sr^{II}, respectively) and exhibits a similar chemistry. In general, Eu^{II} forms complexes with the same types of ligands as the alkaline earth ions and with stability constants similar to Ca^{II} and Sr^{II} [20,21].

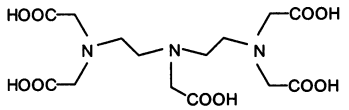

H_5DTPA

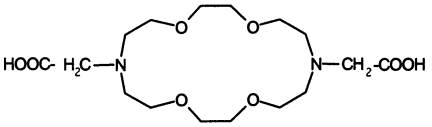

H_2ODDA

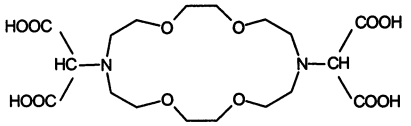

H_4ODDM

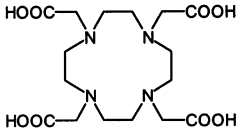

H_4DOTA

Scheme 1.

3. Solid and solution state structure of Eu^{II} complexes

Solid state X-ray structure has been reported only for one Eu^{II} poly(amino carboxylate) complex, the $[Eu^{II}(DTPA)(H_2O)]^{3-}$ [18]. However, due to the similar ionic size and charge, thus similar chemical behavior of Eu^{II} and Sr^{II}, in cases where it is impossible to obtain suitable Eu^{II} crystals, indirect information can be provided by the analogue Sr^{II} compounds. Indeed, experimental data support this practice: the solid state X-ray structures — all bond lengths and angles — found for $[Eu^{II}(DTPA)(H_2O)]^{3-}$ and $[Sr(DTPA)(H_2O)]^{3-}$ are practically identical. The coordination number of both divalent metals is nine, with one inner-sphere water molecule (Fig. 4). The coordination polyhedron is close to a regular capped square antiprism.

The crystal structures of $[Sr(DTPA)(H_2O)]^{3-}$ and $[Eu^{II}(DTPA)(H_2O)]^{3-}$ are also similar to that of the $[Gd(DTPA)(H_2O)]^{2-}$ complex, except for the bond lengths. Due to the lower charge and the larger ionic radius of Sr^{II} and Eu^{II}, the

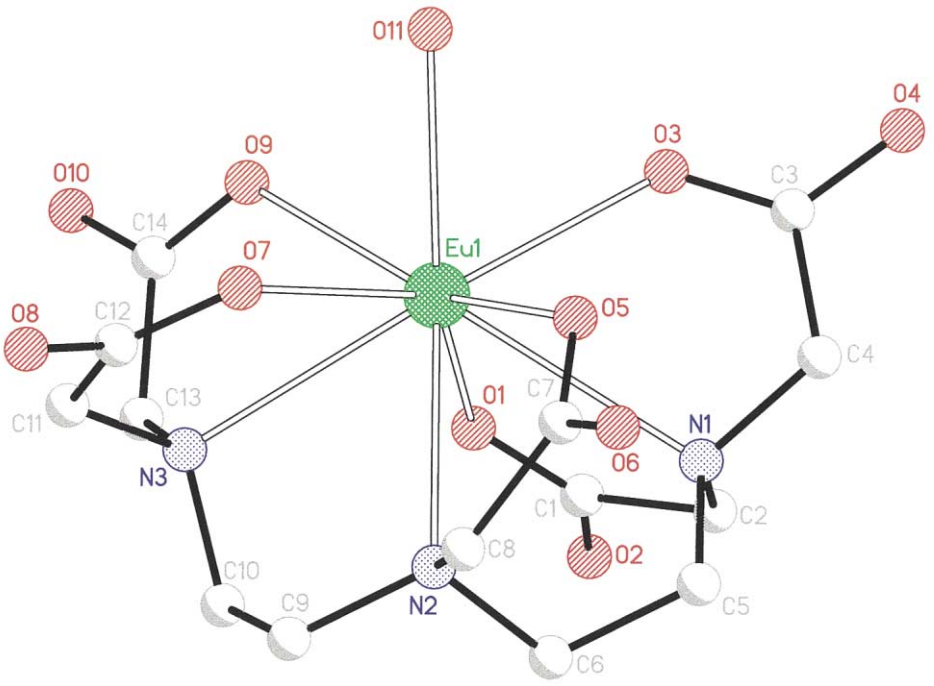

Fig. 4. X-ray structure of $[Eu^{II}(DTPA)(H_2O)]^{3-}$. The O11 represents the oxygen of the inner-sphere water molecule.

metal–oxygen and metal–nitrogen bond lengths are about 0.15 Å longer than those of the corresponding Gd^{III} complex [22]. For example, the distance between the metal center and the coordinated water oxygen ranges from 2.408 to 2.490 Å for Gd^{III} DTPA-type complexes in general [1] (it is 2.490 Å for $[Gd(DTPA)(H_2O)]^{2-}$) [22], while it is 2.619 and 2.622 Å in $[Sr(DTPA)(H_2O)]^{3-}$ and $[Eu^{II}(DTPA)(H_2O)]^{3-}$, respectively. Whereas the bond distances are different, the average angles between the coordinated water molecule and the bound carboxylate oxygens are very similar: 73.4° in $[Gd(HDTPA)(H_2O)]^{-}$ [23] compared to 76.3° in the $[Eu^{II}(DTPA)(H_2O)]^{3-}$ complex and 76.6° for the Sr complex (bond angles are available only for the protonated $[Gd(HDTPA)(H_2O)]^{-}$).

Although the structure of the macrocyclic Eu^{II}(ODDA) complex could be deduced only by analogy from the structure of the corresponding Sr chelate [18], it is worth to shortly discuss since it has a unique feature among poly(amino carboxylate) metal complexes. In solid state, the Sr(ODDA), and presumably, Eu^{II}(ODDA) have a linear polymeric structure without inner-sphere water molecule (Fig. 5). Eight coordination sites of the total nine around the metal ion are occupied by four oxygens and two nitrogens of the macrocyclic ring and one oxygen of each carboxylate group. At the ninth position a carboxylate oxygen coming from a neighbor ligand is coordinated. In aqueous solution, this bond

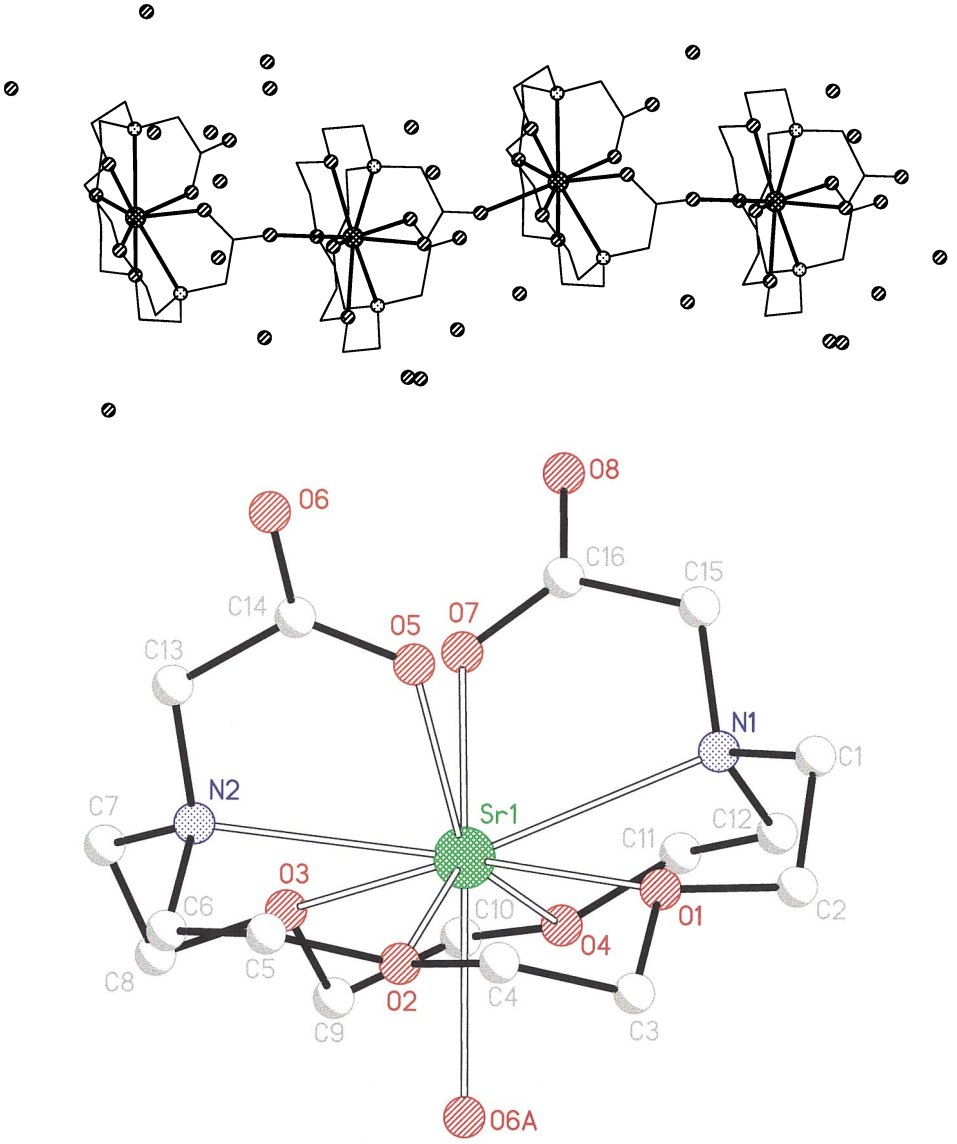

Fig. 5. X-ray structure of Sr(ODDA). The linear polymer chain is shown on the top; the monomer unit is represented by the structure below (the O6A corresponds to a carboxylate of a neighbouring complex).

breaks up and one water molecule enters the inner coordination sphere, as it is evidenced by ^{17}O-NMR for the Eu^{II} complex. In this solution structure the coordination of the inner-sphere water and that of the carboxylates occur on the opposite sides of the molecule. In all poly(amino carboxylate) complexes where

either solid state X-ray data and/or solution structures obtained by molecular dynamics simulation are known, the inner-sphere water coordinates from the carboxylate side of the ligand. Therefore a well-defined hydrophilic region (carboxylates plus inner-sphere water) can be distinguished from a hydrophobic region given by the ligand backbone on the other side of the molecule. Interestingly, this separation of a hydrophobic and hydrophilic side is missing for the $[Sr(ODDA)(H_2O)]$ and $[Eu^{II}(ODDA)(H_2O)]$ complexes.

4. Redox and thermodynamic complex stability of Eu^{II} chelates

An eventual application of the Eu^{III}/Eu^{II} system as a redox responsive switch for MRI requires the sufficient stabilization of the reduced oxidation state. On the other hand, the thermodynamic stability of the complex has to be high enough to avoid toxicity due to the liberation of free metal. Although recently we have gained some insight into the effects influencing redox and thermodynamic stability of Eu^{II} chelates, at the present stage the known Eu^{II} complexes are far from being applicable for biomedical purposes.

Following the general trend, the thermodynamic complex stability constants of the Eu^{II} chelates are very close to those of the Sr^{II} analogues (Table 1). As expected, the stability of $[Eu^{II}(DTPA)(H_2O)]^{3-}$ is far less than that of $[Gd(DTPA)(H_2O)]^{2-}$ ($\log K_{Eu(II)L} = 10.08$ versus $\log K_{GdL} = 22.4$) [21,24].

The redox stability is characterized by the redox potential of the $Eu^{III}L/Eu^{II}L$ couple; a more negative potential meaning lower redox stability against oxidation. For Eu^{II} it is generally accepted that it can be oxidized both by oxygen and water. The redox potentials have been measured for $[Eu^{II}(H_2O)_8]^{2+}$, $[Eu^{II}(DTPA)(H_2O)]^{3-}$, $[Eu^{II}(DOTA)(H_2O)]^{2-}$, $[Eu^{II}(ODDA)(H_2O)]$ and $[Eu^{II}(ODDM)]^{2-}$; the cyclic voltammetry curves obtained are shown in Fig. 6. It is clear from Fig. 6 that the macrocyclic $[Eu^{II}(ODDA)(H_2O)]$, $[Eu^{II}(ODDM)]^{2-}$ and $[Eu^{II}(DOTA)(H_2O)]^{2-}$ complexes are more redox stable than $[Eu^{II}(DTPA)(H_2O)]^{3-}$, the redox potentials are $E_{1/2} = -1.18$, -0.92, and -0.82 V for $[Eu^{II}(DOTA)(H_2O)]^{2-}$, $[Eu^{II}$-

Table 1
Stability and protonation constants ($\log K_{ML}$ and $\log {}^{H}_{ML}$) of the complexes at 25°C

	$ODDM^{4-}$ [a]		$ODDA^{2-}$ [a]		$DTPA^{5-}$	
	Eu^{II}	Sr^{II}	Eu^{II}	Sr^{II}	Eu^{II} [b]	Sr^{II} [c]
$\log K_{ML}$	13.07	11.34	9.85	8.66	10.08	9.68
$\log K^{H}_{ML}$	4.42	4.56	4.97	4.92	5.45	5.4

[a] Ref. [18], in 0.1 M $(CH_3)_4NCl$.
[b] Ref. [21], in 1.0 M KCl.
[c] Ref. [24], in 1.0 M KCl.

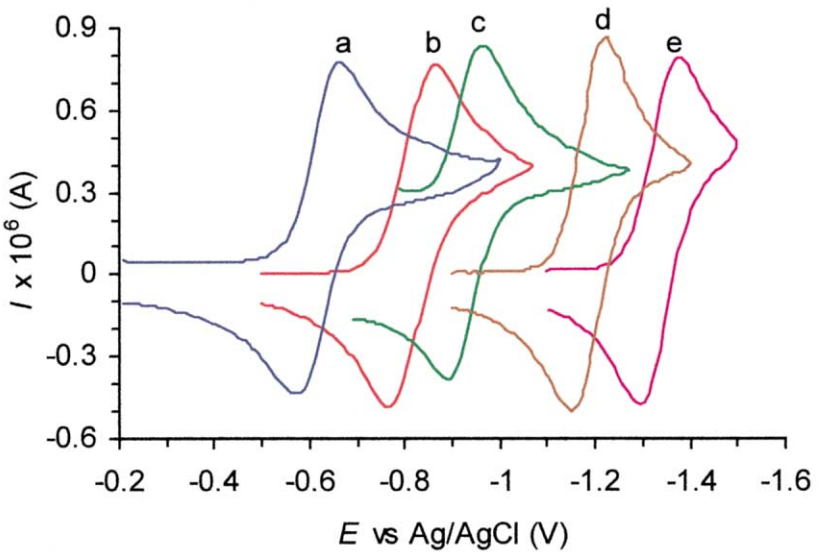

Fig. 6. Cyclovoltammetric curves of aqueous solutions of: (a) $[Eu^{III}(H_2O)_8]^{3+}$; (b) $[Eu^{III}(ODDA)(H_2O)]^{+}$; (c) $[Eu^{III}(ODDM)(H_2O)]^{-}$; (d) $[Eu^{III}(DOTA)(H_2O)]^{-}$; and (e) $[Eu^{III}(DTPA)(H_2O)]^{2-}$.

$(ODDM)]^{2-}$ and $[Eu^{II}(ODDA)(H_2O)]$, respectively, compared to $E_{1/2} = -1.35$ V for $[Eu^{II}(DTPA)(H_2O)]^{3-}$ ($E_{1/2}$ values are given versus Ag | AgCl electrode). However, all complexes studied are less stable against oxidation than the aqua ion, $[Eu^{II}(H_2O)_8]^{2+}$, itself ($E_{1/2} = -0.63$ V).

The kinetics of the oxidation of Eu^{II} also shows the same stability order: the macrocyclic complexes are considerably more inert towards oxidation then $[Eu^{II}(DTPA)(H_2O)]^{3-}$. In all cases the redox stability was found to increase with increasing concentration. Although the number of complexes studied is rather limited to define general trends, carboxylate coordinating groups seem to decrease the stability of Eu^{II} complexes against oxidation in aqueous solution. On the other hand, macrocyclic complexes are likely to be more stable than those formed with linear ligands. Exceptionally high redox stabilities have been reported for Eu^{II} polyoxodiaza cryptates. For all cryptate complexes studied, the redox potentials, $E_{1/2}$, were found to be less negative than that of $[Eu^{II}(H_2O)_8]^{2+}$ [25–27].

Certainly, the redox potential of a given $Eu^{II}L/Eu^{III}L$ couple depends on the relative thermodynamic stabilities of the $Eu^{II}L$ and $Eu^{III}L$ complexes (Eq. (1)). The higher is the stability constant for the complex of the oxidized form $Eu^{III}L$ as compared to that of the reduced form, $Eu^{II}L$, the more negative the redox potential will be. The difference in the potentials between the complexed and uncomplexed one-electron redox couples ($\Delta E_{1/2}$) is directly related to ratio of the stability constants:

$$\Delta E_{1/2} = E_{1/2,\,\text{complexed}} - E_{1/2,\,\text{uncomplexed}} = \frac{RT}{F} \ln \frac{K^{II}}{K^{III}} \quad (1)$$

where K^{III} and K^{II} are the thermodynamic stability constants of the oxidized and reduced forms, respectively. The reason for the Eu^{II} cryptates having high redox stability (more positive reduction potentials) is the thermodynamic instability of the Eu^{III} cryptates, since the cavity size of these ligands matches perfectly to the size of alkaline earth ions, particularly to Sr^{2+} and thus to Eu^{2+} [28].

5. Kinetics of water exchange — comparison of Eu^{II} and Gd^{III} chelates

The water exchange rates, activation enthalpies and entropies as well as the activation volumes for different Gd^{III} and Eu^{II} complexes are shown in Table 2 (since there are no data for $[Gd(ODDA)(H_2O)]^+$ to have a direct comparison, we have chosen $[Gd(DOTA)(H_2O)]^-$ as another representative example of Gd^{III} poly(amino carboxylate complexes). The volumes of activation indicate an associative character of the water exchange mechanism for both eight coordinate aqua ions, $[Gd(H_2O)_8]^{3+}$ and $[Eu^{II}(H_2O)_8]^{2+}$. On $[Eu^{II}(H_2O)_8]^{2+}$ the water exchange is a limiting associative process and has the highest rate ever measured at an aqua ion by magnetic resonance.

The coordination of the octadentate $DTPA^{5-}$ ligand to both Gd^{III} and Eu^{II} results in a change in the water exchange mechanism from the associative to a dissociatively activated process for the metal chelates. For $[Gd(DTPA)(H_2O)]^{2-}$ and for nine-coordinate Gd^{III} poly(amino carboxylate) complexes in general, the change in the mechanism is accompanied by a considerable decrease (several orders of magnitude) in the water exchange rate. In fact, the diminution of the water exchange rate was rationalized in terms of the different mechanisms. The nine-coordinate Gd^{III} poly(amino carboxylates) all have positive activation volumes indicating dissociatively activated water exchange. This is expected since in a nine-coordinate lanthanide complex there is no longer space for a second water molecule to enter before the subsequent departure of the bound water molecule. On the other hand, for most of these complexes the eight-coordinate transition state is

Table 2
Water exchange parameters of the complexes obtained from the variable temperature ^{17}O relaxation rates and ^{1}H-NMRD data

	k_{ex}^{298} (10^9 s^{-1})	$\Delta H^{\#}$ (kJ mol^{-1})	$\Delta S^{\#}$ (J mol^{-1} K^{-1})	$\Delta V^{\#}$ (cm^3 mol^{-1})	Mechanism	Ref.
$[Gd(H_2O)_8]^{3+}$	0.8	15.3	−23.1	−3.3	$\mathbf{I_a}$	[5]
$[Gd(DTPA)(H_2O)]^{2-}$	0.0033	51.6	+53	+12.5	**D**	[5]
$[Gd(DOTA)(H_2O)]^{-}$	0.0041	49.8	+48.5	+10.5	**D**	[5]
$[Eu^{II}(H_2O)_8]^{2+}$	4.4	15.7	−7.0	−11.3	**A**	[16]
$[Eu^{II}(DTPA)(H_2O)]^{3-}$	1.3	26.3	+18.4	+4.5	$\mathbf{I_d}$	[17]
$[Eu^{II}(ODDA)(H_2O)]$	0.43	22.5	−4.0	−3.9	$\mathbf{I_a}$	[18]

energetically unstable, since for them the coordination number of nine is observed all along the lanthanide series [29,30]. The instability of the transition state leads a decreased rate constant. Another important factor is the rigidity of the inner coordination sphere. Whereas in the aqua ion the rearrangement of the flexible coordination sphere occurs easily, the poly(amino carboxylate) complexes have a much more rigid inner-sphere structure whose rearrangement requires higher energy. In conclusion, the difference in the inner-sphere structure, hence the difference in the mechanism is the reason why water exchange on nine-coordinate Ln^{III} poly(amino carboxylate) complexes is generally much slower compared to the eight-coordinate $[Gd(H_2O)_8]^{3+}$.

Contrary to this, the water exchange on $[Eu^{II}(DTPA)(H_2O)]^{3-}$ is only slightly slowed down as compared to $[Eu^{II}(H_2O)_8]^{2+}$. Due to the lower charge and larger ionic radius, the charge density is significantly smaller on the Eu^{II} ion as compared to Gd^{III}. In a dissociatively activated exchange, the rate determining dissociation of the metal–water O bond will be much easier for a metal with low charge density such as Eu^{II}. The longer metal-coordinated water distance is also favorable for the fast water exchange. On the other hand, the water exchange has a definitely less dissociative character for $[Eu^{II}(DTPA)(H_2O)]^{3-}$ ($\Delta V^{\#} = +4.5$ cm^3 mol^{-1}; thus rather $\mathbf{I_d}$) as compared to $[Gd(DTPA)(H_2O)]^{2-}$ ($\Delta V^{\#} = +12.5$ cm^3 mol^{-1}; limiting **D**) indicating less steric crowding around the Eu^{II}, which is also a consequence of its larger size. The lower $\Delta H^{\#}$ and the less positive $\Delta S^{\#}$ values obtained for the Eu^{II} complex are also consistent with a less dissociative water exchange mechanism. Consequently, in the case of $[Eu^{II}(DTPA)(H_2O)]^{3-}$ there is a much stronger participation of the incoming water molecule which is another factor that facilitates the water exchange, thus increases the rate.

The water exchange is 10 times slower on $[Eu^{II}(ODDA)(H_2O)]$ than on $[Eu^{II}(H_2O)_8]^{2+}$. The negative activation volume and the negative activation entropy are evidence for an associatively activated interchange ($\mathbf{I_a}$) mechanism. The difference in the water exchange mechanism on the $[Eu^{II}(ODDA)(H_2O)]$ and $[Eu^{II}(DTPA)(H_2O)]^{3-}$ can be explained in terms of their different structure. The distances between the metal and the coordinating atoms as well as the bond angles show that the water coordinating site is much more open in the ODDA than in the DTPA complex. Consequently, the $[Eu^{II}(ODDA)(H_2O)]$ can accommodate a second water molecule in the inner sphere without the preceding departure of the leaving water molecule leading to an associative activation mode. In the case of $[Eu^{II}(DTPA)(H_2O)]^{3-}$ the inner-sphere water has to leave first in order to provide enough room for the entering molecule. The different mechanisms are likely to account for the difference in the exchange rates as well.

6. Electron spin relaxation

The symmetric electronic ^8S ground state means that Eu^{II} has an observable EPR spectrum in solution. The EPR linewidths of the Eu^{II} complexes, similarly to those of the Gd^{III} analogues, decrease with increasing frequency. This behavior is

consistent with a modulated transient zero field splitting (ZFS) relaxation mechanism [31]. In contrast to Gd^{III}, the EPR spectra of Eu^{II} show fine structure which becomes more apparent as the frequency is increased. Fig. 7 shows typical high frequency (225 GHz) EPR spectra of $[Gd(H_2O)_8]^{3+}$ and $[Eu^{II}(H_2O)_8]^{2+}$.

The EPR spectrum of Eu^{II} can be interpreted as superimposed isotropic hyperfine structures of the ^{151}Eu and ^{153}Eu isotopes, both having a nuclear spin of 5/2 and a similar natural abundance (47.82 and 52.18%, respectively). At the wings of the spectra the outermost lines of ^{151}Eu hyperfine sextet can be recognized, since its nuclear g-factor is larger by a factor of 2.264 than that of ^{153}Eu. In the centre of the spectra the four inner lines of ^{151}Eu and the six-line pattern of ^{153}Eu are superimposed ($\gamma(^{151}Eu) = 6.55 \times 10^7\ T^{-1}\,s^{-1}$ and $\gamma(^{153}Eu) = 2.94 \times 10^7\ T^{-1}\,s^{-1}$). In the case of Gd^{III}, no hyperfine structure is observed even at high magnetic field (see Fig. 7), since the two isotopes with non-zero nuclear spin have relatively low γ and low abundance. For the Eu^{II} poly(amino carboxylate) complexes studied the linewidths are considerably larger than for the aqua ion, indicating a higher electron spin relaxation rate.

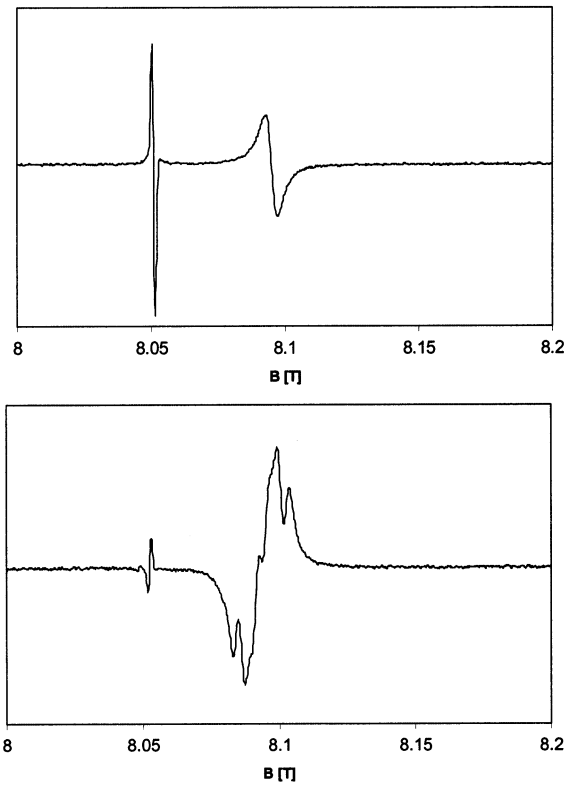

Fig. 7. Typical high-frequency (225 GHz) EPR spectra of $[Gd(H_2O)_8]^{3+}$ ($c = 0.080$ M) and $[Eu^{II}(H_2O)_8]^{2+}$ ($c = 0.176$ M). The low-field peak is the signal of the BDPA used as a g-factor reference (BDPA = a,g-bisdiphenyline-b-phenylallyl).

The parameters that define electronic relaxation are the square of the trace of the ZFS tensor, Δ^2, and the correlation time which describes the modulation of the transient ZFS distortion, τ_v (Table 3). The value of Δ^2 obtained for $[Eu^{II}(H_2O)_8]^{2+}$ is close to that for $[Eu^{II}(ODDA)(H_2O)]$ and $[Gd(H_2O)_8]^{3+}$ indicating similar magnitude of the transient ZFS distortion. The considerably shorter τ_v for $[Eu^{II}(H_2O)_8]^{2+}$ means that the transient ZFS is modulated at a faster rate. As the result of this faster modulation, the transient ZFS distortions are better averaged for $[Eu^{II}(H_2O)_8]^{2+}$ than for the poly(amino carboxylate) complexes or for $[Gd(H_2O)_8]^{3+}$ which leads to a longer value of T_{1e} and T_{2e} for the Eu^{II} aqua ion. Based on these few examples, it seems that the formation of Eu^{II} poly(amino carboxylate) complexes results in faster electronic relaxation as compared to the aqua ion. It is in contrast to Gd^{III} chelates, where, in general, electron spin relaxation is slower on the complexes than on the aqua ion itself (at least at magnetic fields important for magnetic resonance imaging).

7. Proton relaxivity

A comparison of the NMRD profiles obtained at 298 K for the two aqua ions, $[Gd(H_2O)_8]^{3+}$ and $[Eu^{II}(H_2O)_8]^{2+}$, as well as for $[Gd(DTPA)(H_2O)]^{2-}$, $[Eu^{II}(DTPA)(H_2O)]^{3-}$, $[Eu^{II}(ODDA)(H_2O)]$ and $[Gd(ODDA)(H_2O)]^{+}$ are shown in Figs. 8–10. The lines represent a fit to the experimental points according to the usual theory applied for paramagnetic complexes (for clarity, we present the profiles only at one temperature, however, the fit has been performed using data points at several different temperatures) [5,16–18]. It is well known that for the Gd^{III} aqua ion and for monomer Gd^{III} poly(amino carboxylates) in general, thus for $[Gd(DTPA)(H_2O)]^{2-}$, fast rotation limits proton relaxivity at imaging fields (20–60 MHz proton Larmor frequency). Consequently, it is not surprising that the corresponding Eu^{II} complexes — having similar rotational correlation times — have not higher proton relaxivity, either. However, the analysis of the NMRD profiles of $[Eu^{II}(H_2O)_8]^{2+}$ reveals that beside rotation, fast water exchange, which is already faster than the optimal value (see Fig. 3) also becomes a limiting factor.

Table 3
Electron spin relaxation parameters of the complexes

	τ_v^{298} (ps)	E_v (kJ mol^{-1})	Δ^2 ($10^{20} \times s^{-2}$)	Ref.
$[Gd(H_2O)_8]^{3+}$	7.3	18.4	1.19	[5]
$[Gd(DTPA)(H_2O)]^{2-}$	25	1.6	0.46	[5]
$[Gd(DOTA)(H_2O)]^{-}$	11	1.0	0.16	[5]
$[Eu^{II}(H_2O)_8]^{2+}$	1.0	12.5	1.13	[16]
$[Eu^{II}(DTPA)(H_2O)]^{3-}$	13.6	1	1.7	[17]
$[Eu^{II}(ODDA)(H_2O)]$	14.3	1	1.01	[18]

For $[Eu^{II}(DTPA)(H_2O)]^{3-}$ and $[Eu^{II}(ODDA)(H_2O)]$, the water exchange rate is in the optimal range to obtain maximum relaxivities. In these cases the fast rotation of the small molecular weight complex prevents the proton relaxivity from attaining higher values. We have seen above that electron spin relaxation is considerably faster on the Eu^{II} poly(amino carboxylates) than on the aqua ion. This fast electron spin relaxation will have an effect on the proton relaxivities as well: between 20 and 60 MHz they are limited not only by fast rotation, but also by fast electron spin relaxation. In the case of Gd^{III} complexes, it has been proposed only for com-

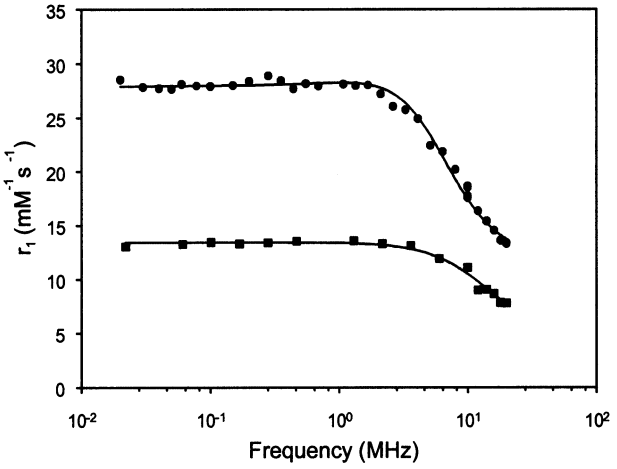

Fig. 8. NMRD profiles of $[Gd(H_2O)_8]^{3+}$ (●) and $[Eu^{II}(H_2O)_8]^{2+}$ (■), $T = 298$ K.

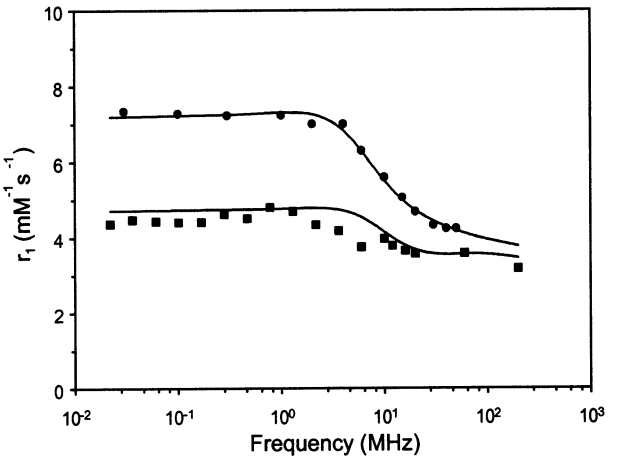

Fig. 9. NMRD profiles of $[Gd(DTPA)(H_2O)]^{2-}$ (●) and $[Eu^{II}(DTPA)(H_2O)]^{3-}$ (■), $T = 298$ K.

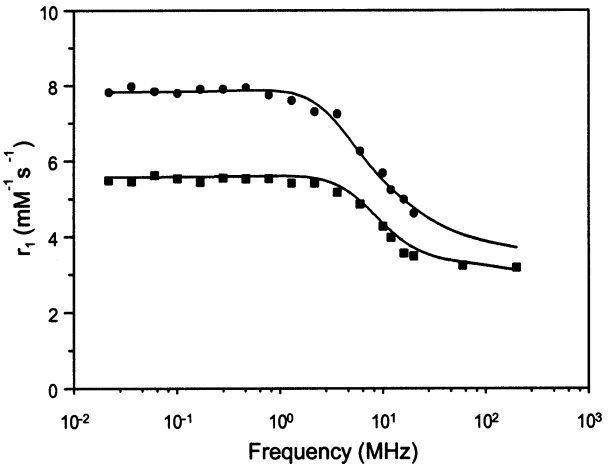

Fig. 10. NMRD profiles of $[Gd(ODDA)(H_2O)]^+$ (●) and $[Eu^{II}(ODDA)(H_2O)]$ (■), $T = 298$ K.

pounds with long (at least nanosecond) rotational correlation times that electronic relaxation can limit proton relaxivity at medium fields (20 MHz), though no example has been reported so far. This is mainly due to the fact that electronic relaxation is relatively slow for Gd^{III} complexes (which is a great advantage of this paramagnetic metal ion over others in MRI applications), hence slow water exchange starts to limit the relaxivity of these slowly rotating agents before one could see the effect of the electronic relaxation. These Eu^{II} chelates are the first examples where the limitation of electron spin relaxation is observed even with fast rotation, at magnetic fields important for MRI application (20–60 MHz proton Larmor frequency). By increasing the rotational correlation time, the limiting effect of electronic relaxation would evidently become much more important. This could mean that fast electron spin relaxation can be an obstacle to the potential application of Eu^{II} chelates as contrast agents in magnetic resonance imaging. However, preliminary EPR experiments on other Eu^{II} complexes indicate that this unfavourable property is not general.

8. Conclusions

The solid state X-ray structures — all metal–nitrogen and metal–oxygen bond lengths and angles — of the $[Eu^{II}(DTPA)(H_2O)]^{3-}$ and of the analogue Sr^{II} complex are practically identical. Furthermore, the bond angles are equal to those reported for $[Gd(DTPA)(H_2O)]^{2-}$, whereas the bond distances between the metal and the coordinating atoms are somewhat longer for $[Eu^{II}(DTPA)(H_2O)]^{3-}$ as a consequence of the lower charge and larger ionic radius of the divalent metal ion. In aqueous solution, the stability of Eu^{II} against oxidation is higher in complexes

formed with macrocyclic ligands than in $[Eu^{II}(DTPA)(H_2O)]^{3-}$, but still lower than in the aqua complex. Carboxylate coordinating groups seem unfavourable for the redox stability of the Eu^{II} state. Certain Eu^{II} cryptates have very high redox stability, since their cavity size fits well to Eu^{II} but it is too large for Eu^{III}, resulting in an instability of the Eu^{III} complex. The redox potential of the Eu^{II}/Eu^{III} couple is related to the ratio of the stability constants of the $Eu^{II}L$ (similar to SrL) and $Eu^{III}L$ complexes. Thus in general, in order to find favorable redox potentials, one has to compare the stability constants between SrL and $Eu^{III}L$. The smaller this difference, the more redox stable will be the $Eu^{II}L$ state. However, for any biomedical application, not only the ratio of the stability constants has to be considered, but their absolute values have also to be sufficiantly high in order to avoid the liberation of free metal.

The water exchange rate on the Eu^{II} aqua ion is the fastest ever measured by magnetic resonance. For the nine-coordinate $[Eu^{II}(DTPA)(H_2O)]^{3-}$ and $[Eu^{II}(ODDA)(H_2O)]$ complexes the water exchange rate is only slightly decreased as compared to the Eu^{II} aqua ion, whereas for similar Gd^{III} chelates a considerable diminution of the exchange rate has been observed. The mechanism of water exchange is dissociative interchange for $[Eu^{II}(DTPA)(H_2O)]^{3-}$ and associative interchange for $[Eu^{II}(ODDA)(H_2O)]$. This difference can be rationalized in terms of their different inner-sphere structure: due to the less steric crowding, the $[Eu^{II}(ODDA)(H_2O)]$ can accommodate a second water molecule without the departure of the first one. The electron spin relaxation for $[Eu^{II}(ODDA)(H_2O)]$ and $[Eu^{II}(DTPA)(H_2O)]^{3-}$ is faster than for Gd^{III} chelates in general, and, beside fast rotation, limits their proton relaxivity even at imaging magnetic fields. Therefore, in order to take advantage of the optimal water exchange rate of Eu^{II} chelates and thus to obtain high relaxivities, macromolecular Eu^{II} complexes with slower electron spin relaxation are required.

At the present stage, the in vivo applicability of Eu^{II} complexes as MRI redox reporters remains questionable, mainly due to the difficulties in the control of the reduced state. Efforts are focused on the synthesis of new water soluble macrocyclic ligands with matching cavity size for Eu^{2+} in order to ensure high thermodynamic and redox stability of the Eu^{II} chelate.

Acknowledgements

We thank Lothar Helm for the helpful discussions. We are grateful to the Swiss National Science Foundation and the Office for Education and Science (OFES) for their financial support. This research was carried out in the frame of the EC COST D18 Action "Lanthanide Complexes in Biology and Medicine".

References

[1] P. Caravan, J.J. Ellison, T.J. McMurry, R.B. Lauffer, Chem. Rev. 99 (1999) 2293.
[2] S.H. Koenig, R.D. Brown III, Prog. Nucl. Magn. Reson. Spectrosc. 22 (1990) 487.

[3] A. Borel, L. Helm, A.E. Merbach, Chem. Eur. J. 7 (2001) 600.
[4] S.H. Koenig, J. Magn. Res. 31 (1978) 1.
[5] H.D. Powell, O.M. Ni Dhubhghaill, D. Pubanz, L. Helm, Y. Lebedev, W. Schlaepfer, A.E. Merbach, J. Am. Chem. Soc. 118 (1996) 9333.
[6] E.C. Wiener, M.W. Brechbiel, H. Brothers, R.L. Magin, O. Gansow, D.A. Tomalia, P.C. Lauterbur, Magn. Res. Med. 31 (1994) 1.
[7] R.B. Lauffer, D.J. Parmelee, S.U. Dunham, H.S. Ouellet, R.P. Dolan, S. Witte, T.J. McMurry, R.C. Walowitch, Radiology 207 (1998) 529.
[8] É. Tóth, L. Helm, K.E. Kellar, A.E. Merbach, Chem. Eur. J. 5 (1999) 1202.
[9] É. Tóth, D. Pubanz, S. Vauthey, L. Helm, A.E. Merbach, Chem. Eur. J. 2 (1996) 1607.
[10] É Tóth, L. Burai, E. Brücher, A.E. Merbach, J. Chem. Soc. Dalton Trans. (1997) 1587.
[11] J.P. André, H.R. Maecke, É. Tóth, A.E. Merbach, J. Biol. Inorg. Chem. 4 (1999) 341.
[12] E. Szilágyi, É. Tóth, E. Brücher, A.E. Merbach, J. Chem. Soc. Dalton Trans. (1999) 2481.
[13] É. Tóth, O.M. Ni Dhubhghaill, G. Besson, L. Helm, A.E. Merbach, Magn. Res. Chem. 37 (1999) 701.
[14] R.A. Moats, S.E. Fraser, T.J. Meade, Angew. Chem. Int. Ed. Engl. 36 (1997) 726.
[15] S. Aime, M. Botta, E. Gianolio, E. Terreno, Angew. Chem. Int. Ed. Engl. 39 (2000) 747.
[16] P. Caravan, É. Tóth, A. Rockenbauer, A.E. Merbach, J. Am. Chem. Soc. 121 (1999) 10403.
[17] S. Seibig, É. Tóth, A.E. Merbach, J. Am. Chem. Soc. 122 (2000) 5822.
[18] L. Burai, É. Tóth, S. Seibig, R. Scopelliti, A.E. Merbach, Chem. Eur. J. 6 (2000) 3761.
[19] E. Brücher, B. Györi, J. Emri, S. Jakab, P. Solymosi, I. Tóth, J. Chem. Soc. Dalton Trans.(1995) 3353.
[20] D.A. Johnson, Adv. Inorg. Chem. Radiochem. 20 (1977) 1.
[21] G. Laurenczy, E. Brücher, Proceedings of the International Symposium on Rare Earth Spectroscopy, Wroclaw, 1984, p. 127.
[22] H. Gries, H. Miklautz, Physiol. Chem. Phys. Med. NMR 16 (1984) 105.
[23] R. Ruloff, T. Gelbrich, E. Hoyer, J. Sieler, L. Beyer, Z. Naturforsch. 53b (1998) 955.
[24] A.E. Martell, R.M. Smith, Critical Stability Constants, vol. vol. 1, Plenum Press, New York, 1974 (p. 281).
[25] E.L. Yee, O.A. Gansow, M.J. Weaver, J. Am. Chem. Soc. 102 (1980) 2278.
[26] M.C. Almasio, F. Arnaud-Neu, M.J. Schwing-Weill, Helv. Chim. Acta 66 (1983) 1296.
[27] J. Jiang, N. Higashiyama, K. Machida, G. Adachi, Coord. Chem. Rev. 170 (1998) 1.
[28] J.-M. Lehn, Acc. Chem. Res. 11 (1978) 49.
[29] J.A. Peters, Inorg. Chem. 27 (1988) 4686.
[30] C.F.G.C. Geraldes, A.D. Sherry, W.P. Cacheris, K.-T. Kuan, R.D. Brown III, S.H. Koenig, M. Spiller, Magn. Res. Med. 8 (1988) 191.
[31] L. Banci, I. Bertini, C. Luchinat, Nuclear and Electron Relaxation, VCH, New York, 1991.